

## Satellite structure of the xenon valence shell by electron-momentum spectroscopy

S. Braidwood, M. Brunger, and Erich Weigold

*Electronic Structure of Materials Centre, School of Physical Sciences, Flinders University of South Australia,  
G.P.O. Box 2100, Adelaide, 5001, South Australia*

(Received 29 May 1992)

Momentum distributions and spectroscopic factors are obtained in a high-resolution electron-momentum spectroscopy study of xenon at 1000 eV. The shapes and relative magnitudes of the momentum profiles are in excellent agreement with distorted-wave (DW) impulse approximations using the target Dirac-Fock (DF) approximation. The DWDF approximation accurately describes the relative magnitudes of the  $5p$  and  $5s$  manifold cross sections as well as the shape of the  $5s$  cross section. The use of nonrelativistic Hartree-Fock wave functions gives significantly poorer fits to the data. Spectroscopic factors for transitions belonging to the  $^2S_{1/2}^e$ ,  $^2P_{1/2,3/2}^o$ , and  $^2D_{3/2,5/2}^e$  manifolds are assigned up to a separation energy of 45 eV. The spectroscopic strength for the lowest  $5s$  transition is  $0.345 \pm 0.010$  whereas that for the ground-state  $5p$  transition is  $0.96 \pm 0.02$ . The  $5s$  strength in the continuum above 33.1 eV is  $0.115 \pm 0.025$  and that for the  $5p$  manifold is only  $0.03 \pm 0.01$ . The first momentum profiles belonging to excited  $^2P^o$  and  $^2D^e$  manifolds are obtained. The latter, which must be entirely due to  $d$ -wave correlations in the xenon ground state, are in good agreement with DF  $5d$  momentum profiles. Comparison is made with several many-body calculations and agreement with the latest relativistic calculation is good.

PACS number(s): 34.80.Dp, 35.10.Hn, 31.20.Tz

### I. INTRODUCTION

The valence electronic structure of the rare gases and their ions has been a central problem in atomic structure for some time. This is particularly true for argon and xenon, for which a large number of electron-momentum spectroscopy (EMS) studies (e.g., Refs. [1–5]) and photoelectron spectroscopy (PES) measurements (e.g., Refs. [6–10]) have been carried out. There have also been many different theoretical calculations reported for the electron separation energy spectra of both argon [10–16] and xenon [16–20].

Much of this work has focused on the ionization of the outer-shell  $s$  electrons, since this is a process of particular interest in studying atomic many-electron correlations. It is generally believed that at high energies the observed electron separation-energy spectrum should not depend on the ionization mechanism and that it can be described mainly by many-electron correlations in the final state of the ion. In this approximation relative line intensities in the separation-energy spectra are equal to the spectroscopic factors or pole strengths of the corresponding ion states, which determine the probability of finding the ion in the pure one-hole state [1]. However, inconsistencies exist between PES measurements at different energies and between the PES and EMS data. The EMS data [1–5] are consistent among each other, giving satellite intensities and structure information independent of incident energy. In general the PES measurements are quite energy dependent and measure a higher spectroscopic factor for the “main”  $ns^{-1}$  transition than that obtained by EMS.

Part of this difference in spectroscopic strengths is due to the inherent difficulty in PES of measuring the strength in the continuum [21], whereas there is in princi-

ple no difficulty in this for EMS. The accuracy obtained in determining the continuum contribution in EMS depends only on the statistical accuracy of the true and accidental coincidence count rates at the relevant binding energies, and on the accuracy of the ratio of the true to accidental window widths [1]. However, the main difference between EMS and PES is probably due to the influence of the atomic ground-state many-electron correlations. Amusia and Kheifets [11,15,20] and Kheifets [22], in a series of Green’s-function calculations, show that these correlations give a contribution to the ionization amplitude that is different for the ground and excited ion states for any symmetry manifold and can potentially change the relative intensities of the main and satellite lines in the separation-energy spectrum. For EMS, where the momentum transferred to the ion is small, these effects are negligible and the relative line intensities correspond to the spectroscopic factors. However, for the case of photoionization, where the momentum transferred to the ion is large, these ground-state correlation effects are of the same order of magnitude as the direct ionization amplitude. The resulting PES line intensities therefore deviate significantly from the standard spectroscopic factors defined as the contribution of the pure one-hole state to the corresponding exact states of the ion.

Amusia and Kheifets find good agreement with their Green’s-function calculations of the pole strengths (spectroscopic factors) with the EMS data for argon [15] and quite good agreement in the case of xenon [20]. They also find that if the spectroscopic factors are corrected by the inclusion of the high-momentum components of the ground-state correlation effects, good agreement is obtained with the PES results. The most significant changes of intensity in the PES spectra are in the main

transition and in the continuum spectrum. Kheifets and Amusia concluded that since the PES probes the very-high-momentum part of the many-electron wave function, it does not obtain correct spectroscopic factors. EMS, on the other hand, obtains true spectroscopic factors since it probes the low-momentum region of the wave function, corresponding to the outer region in coordinate space where the electron probability density is high for valence electrons.

A recent EMS study of argon [2] obtained accurate values of the spectroscopic factors for final states belonging to the  $^2S^e$  and  $^2P^o$  manifolds. It also obtained the momentum profile for an excited state belonging to the  $^2D^e$  manifold. This transition is due to  $d$ -wave correlations in the initial state. For xenon two detailed EMS investigations have been carried out. The first, by Cook, Mitroy, and Weigold [23], showed the importance of relativistic effects in the  $5p_{3/2,1/2}$  momentum profiles. The second, by Cook *et al.* [5], provided a detailed analysis of the  $5s$  manifold in the valence region. However, none of the previous measurements on xenon were accurate enough to measure spectroscopic factors of excited states belonging to manifolds other than the  $5s$  manifold.

In the present work we report an accurate 1000-eV EMS study of the valence electronic structure of xenon, which not only obtains more accurate results for the  $5s$ ,  $J^\pi = \frac{1}{2}^+$  manifold, but also identifies states belonging to the  $5p$  ( $J^\pi = \frac{1}{2}^-, \frac{3}{2}^-$ ) and  $5d$  ( $J^\pi = \frac{3}{2}^+, \frac{5}{2}^+$ ) manifolds. The latter transitions can only occur if there are  $d$ -wave correlations in the initial ground state of xenon. The spectroscopic data for the different manifolds are also compared with the latest theoretical results.

## II. EXPERIMENTAL METHODS

The electron-coincidence spectrometer and the techniques used have been described in some detail previously

[1,5], and only a brief outline need be given here. The only major change to the noncoplanar symmetric coincidence spectrometer has been the inclusion of a differentially pumped collision chamber. The xenon is admitted into the target chamber through a capillary tube, the leak rate being controlled by a variable leak valve. The collision region is surrounded by a chamber pumped by a 700-liter/s diffusion pump. Apertures and slits are cut in the collision chamber for the incident beam and ejected electrons. With the differentially pumped collision region it was possible to increase the gas target density by a factor of 2 while keeping the background pressure in the spectrometer below  $10^{-5}$  torr. This allowed us to operate the electron beam at a lower current (typically 50  $\mu$ A), resulting in better energy resolution. The energy resolution of the spectrometer is limited by the energy spread of the incident beam due to space-charge effects. The energy resolution in the present measurements is 1.06 eV full width at half maximum (FWHM), and the angular resolution is  $1.2^\circ$  FWHM.

Operating conditions were chosen so that the incident energy  $E_0 = 1000$  eV + separation energy, the ejected electrons had energies  $E_A$  and  $E_B$  in the range  $500 \pm 7$  eV and made angles of  $45^\circ$  with respect to the incident direction. The out-of-plane azimuthal angle was varied over the angular range  $0^\circ - 20^\circ$  in order to vary the recoil momentum. Separation-energy spectra were taken at each out-of-plane azimuthal angle over the range 10–45 eV using the binning mode [1].

## III. THEORETICAL BACKGROUND

In the distorted-wave impulse approximation (DWIA) the  $(e, 2e)$  differential cross section from the target ground state  $|0\rangle$  to the final many-electron state  $|f\rangle$  is [1]

$$\frac{d^5\sigma}{d\hat{\mathbf{p}}_A d\hat{\mathbf{p}}_B dE_A} = (2\pi)^4 \frac{P_A P_B}{P_0} f_{ee} \left| \int d^3\mathbf{q} \langle \chi^{(-)}(\mathbf{p}_A) \chi^{(-)}(\mathbf{p}_B) | \mathbf{q} \chi^{(+)}(\mathbf{p}_0) \rangle \langle f | a(\mathbf{q}) | 0 \rangle \right|^2. \quad (1)$$

Here  $f_{ee}$  is the  $e$ - $e$  collision factor, which in the out-of-plane symmetric kinematics is essentially independent of the ion-recoil momentum

$$\mathbf{p} = \mathbf{p}_0 - \mathbf{p}_A - \mathbf{p}_B, \quad (2)$$

$\chi^{(\pm)}(\mathbf{p})$  are distorted waves describing the fast incoming and emitted electrons, and  $a(\mathbf{q})$  is an operator annihilating an electron of momentum  $\mathbf{q}$ .

In the weak-coupling approximation for the target-ion overlap, ion states are described by an expansion in orthonormal basis states which are linear combinations of configurations formed by annihilations of one electron in the target eigenstate. The target eigenstate may of course

be expressed in the configuration-interaction (CI) representation. Generally the weak-coupling expansion of the ion state  $|f\rangle$  contains only a single-hole state  $|i\rangle$  and then [1]

$$\begin{aligned} \langle f | a(\mathbf{q}) | 0 \rangle &= \langle f | i \rangle \langle i | a(\mathbf{q}) | 0 \rangle \\ &= \langle f | i \rangle \psi_i(\mathbf{q}), \end{aligned} \quad (3)$$

where we have defined the experimental orbital  $\psi_i(\mathbf{q})$  by

$$\psi_i(\mathbf{q}) \equiv \langle i | a(\mathbf{q}) | 0 \rangle. \quad (4)$$

The differential cross section is then given by

$$\frac{d^5\sigma}{d\hat{\mathbf{p}}_A d\hat{\mathbf{p}}_B dE_A} = (2\pi)^4 \frac{P_A P_B}{p_0} f_{ee} S_f^{(i)} \left| \int d^3\mathbf{q} \langle \chi^{(-)}(\mathbf{p}_A) \chi^{(-)}(\mathbf{p}_B) | \psi_i(\mathbf{q}) \chi^{(+)}(\mathbf{p}_0) \rangle \right|^2, \quad (5)$$

where the spectroscopic factor

$$S_f^{(i)} = |\langle f | i \rangle|^2 \quad (6)$$

is the probability of the ion state  $|f\rangle$  containing the one-hole state  $|i\rangle$ .

The spectroscopic sum rule

$$\sum_f S_f^{(i)} = \sum_f \langle i | f \rangle \langle f | i \rangle = 1 \quad (7)$$

enables the normalization of the spectroscopic factors or pole strengths, which are proportional to the cross sections for different states  $f$  in the manifold  $i$ . If the ground state  $|0\rangle$  can be represented by the Hartree-Fock (HF) [or Dirac-Fock (DF)] representation, then  $\psi_i(\mathbf{q}) = \phi_i(\mathbf{q})$ , the Hartree-Fock orbital. This is the well-known target Hartree-Fock approximation (THFA) or target Dirac-Fock (TDFA) approximation.

The energy  $\varepsilon_i$  for the one-hole configuration  $i$ , the energy of orbital  $\psi_i$ , is given by

$$\begin{aligned} \varepsilon_i &= \langle i | H_{\text{ion}} | i \rangle = \sum_f \langle i | f \rangle \langle f | H_{\text{ion}} | f \rangle \langle f | i \rangle \\ &= \sum_f S_f^{(i)} \varepsilon_f. \end{aligned} \quad (8)$$

The "orbital" energy  $\varepsilon_i$  is thus the centroid of the energies  $\varepsilon_f = E_0 - E_A - E_B$  of the ion states in the manifold  $i$ .

In the plane-wave impulse approximation where the distorted waves  $\chi^{(+)}(\mathbf{p})$  are replaced by plane waves,  $\mathbf{q} = -\mathbf{p}$  and

$$\frac{d^5\sigma}{d\hat{\mathbf{p}}_A d\hat{\mathbf{p}}_B dE_A} = (2\pi)^4 \frac{P_A P_B}{p_0} f_{ee} S_f^{(i)} (4\pi)^{-1} \int d\hat{\mathbf{q}} |\psi_i(\mathbf{q})|^2, \quad (9)$$

where the spherical average is due to the random orientation of the target atoms or molecules in a gas target.

In the present work we use the DWIA [Eq. (5)] in conjunction with the THFA (or TDFA) for detailed comparison of the data with theory. The differential cross-section calculations are those of Cook *et al.* [5].

## IV. RESULTS AND DISCUSSION

### A. Separation-energy spectrum

The separation-energy spectrum for xenon in the range 20–45 eV is shown in Fig. 1 for a total energy of 1000 eV and with the out-of-plane azimuthal angles of  $0^\circ$  and  $7.5^\circ$ , respectively. At  $\phi = 0^\circ$  the momentum  $p$  ranges from 0.10 a.u. for the first peak at  $\varepsilon_f = 23.4$  eV to 0.17 a.u. at  $\varepsilon_f = 40$  eV. At  $7.5^\circ$  the corresponding momenta are 0.57 and 0.59 a.u. The spectra shown in Fig. 1 are better resolved than those in earlier published EMS works [3–5].

For the sake of clarity the  $5p_{3/2,1/2}^{-1}$  ground-state transitions at 12.13 and 13.43 eV are not shown in the figure. The present measured  $5p_{3/2}:5p_{1/2}$  branching ratio of  $2.308 \pm 0.035$  at  $\phi = 7.5^\circ$  ( $p = 0.56$  a.u.) is in excellent agreement with the ratio given by the DWIA-TDFA calculation of Cook *et al.* [5] as well as with their measured ratios. At  $\phi = 0^\circ$  (i.e., low momentum) the  $5p$  ground-state cross section is only 0.2 of the total  $5s$  manifold  $\phi = 0^\circ$  cross section. At  $\phi = 7.5^\circ$  it is 3.71 times the  $\phi = 7.5^\circ$   $5s$  manifold cross section. Thus any  $5p$  satellite

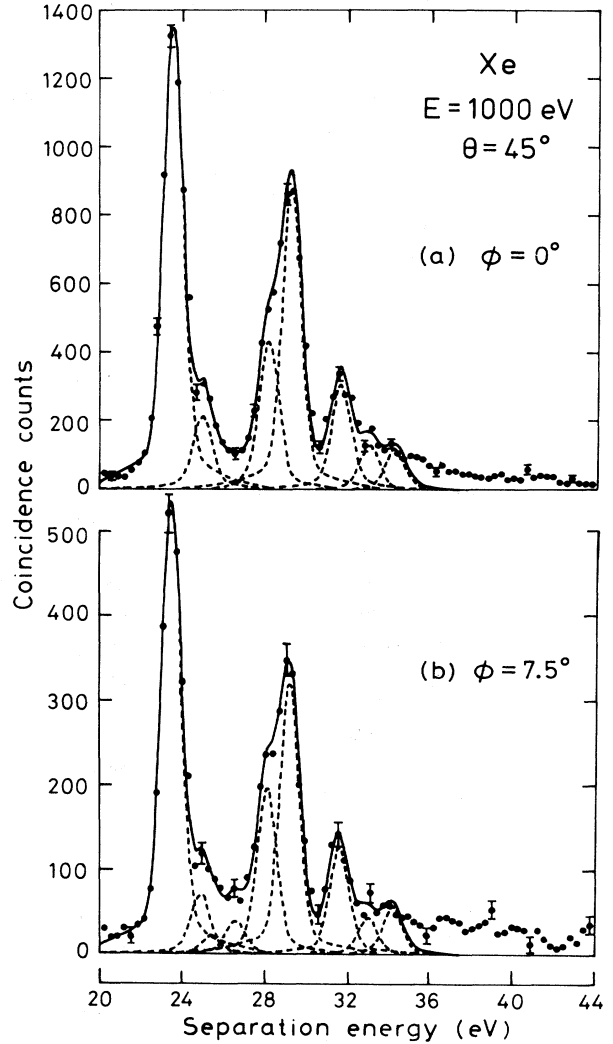


FIG. 1. The 1000-eV noncoplanar symmetric EMS separation-energy spectra for xenon at  $\phi = 0^\circ$  ( $p \sim 0.1$ – $0.17$  a.u.) and  $\phi = 7.5^\circ$  ( $p \sim 0.57$  a.u.). The curves show the fitted spectra using the known energy resolution function. The assignments for the peaks are given in Table I.

intensity in the energy range above 23.4 eV would be much more prominent at  $\phi=7.5^\circ$  than at  $\phi=0^\circ$ .

The relative intensities of the various transitions and their centroid energies are given in Table I. The intensities have been normalized relative to the value of 100 for the 23.4-eV  $5s5p^6\ ^2S_{1/2}$  transition at  $\phi=0^\circ$ . The  $\phi=0^\circ$   $5p^{-1}$  ground-state intensity is a sensitive function of the angular resolution, and is therefore not included in the table.

It is obvious from the relative intensities at  $\phi=0^\circ$  ( $p\sim 0.1$  a.u.) and  $\phi=7.5^\circ$  ( $p\sim 0.57$  a.u.) that the region from 23.4 to 45 eV is dominated by transitions belonging to the  $5s$  manifold. These transitions are significantly more intense, by a factor of approximately 2.5, at  $\phi=0^\circ$  than at  $\phi=7.5^\circ$ . This is due to the  $5s^{-1}$  momentum density, which peaks at  $p=0$ . There is, however, a region between 24.7 and 28.0 eV where the intensity is greater at  $7.5^\circ$  than at  $0^\circ$ . This intensity cannot therefore belong to the  $5s$  manifold. High-resolution syn-

chrotron [8] and x-ray photoelectron spectra [6] show a satellite peak at 25.3 eV of the same intensity as the 24.67 eV transition. Furthermore, they also show a transition at 26.6 eV with similar intensity. In several high-resolution low-energy PES measurements [24–26] the intensities around 25.3 and 26.7 eV significantly exceed that around 24.67 eV. This is clearly not the case in the present work (see Fig. 1 and Table I), which again implies that the transitions at 25.3 and 26.6 eV cannot belong to the  $5s$  manifold. Previous PES experiments [6,18,19,27] have assigned the 25.3-eV transition to the  $5s$  manifold. The present data imply that the spectroscopic factor for an  $s$  contribution to the satellite at this energy would necessarily be very small. This latter observation is not, however, inconsistent with the observed PES line intensities [27], particularly at low photon energies, which, as discussed above, are expected to deviate significantly from the standard spectroscopic factors. The 26.6-eV transition has also mistakenly been assigned to the  $5s$

TABLE I. Relative intensities and assignments for transitions in the valence region of xenon normalized to the value of 100 for the  $5s5p^6\ ^2S_{1/2}$  transition at 23.4 eV and  $\phi=0^\circ$ .

Assignment <sup>a</sup>		EMS relative intensities and peak energies		
Dominant configuration	Energy (eV)	$\epsilon_f$ (eV)	$\theta=0^\circ$	$\theta=7.5^\circ$
$5s^25p^5\ ^2P_{3/2}^o$	12.13	12.13		108.8
$5s^25p^5\ ^2P_{1/2}^o$	13.43	13.43		47.2
$5s5p^6\ ^2S_{1/2}^e$	23.40	23.40	100	39.4
$5s^25p^4(^3P)6s\ ^4P_{1/2}^e$	24.67	24.7	20.7	8.2
$5s^25p^4(^3P)5d\ ^2D_{3/2}^e$	25.19			
$5s^25p^4(^1D)6s\ ^2D_{5/2}^e$	25.71	25.3	1.1	1.6
$5s^25p^4(^1D)6s\ ^2D_{3/2}^e$	26.13			
$5s^25p^4(^1D)5d\ ^2D_{5/2}^e$	26.35			
$5s^25p^4(^3P)6p\ ^2P_{1/2}^o$	26.23	26.5	1.2	2.9
$5s^25p^4(^3P)6p\ ^2P_{3/2}^o$	26.61			
$5s^25p^4(^1D)5d\ ^2P_{1/2}^e$	27.88			
$5s^25p^4(^1S)6s\ ^2S_{1/2}^e$	28.15	28.0	32.2	14.4
$5s^25p^4(^1D)6p\ ^2P_{3/2}^o$	28.21			
$5s^25p^4(^1D)6p\ ^2P_{1/2}^o$	28.59			
$5s^25p^4(^1D)5d\ ^2S_{1/2}^e$	28.87			
$5s^25p^4(^3P)6d\ ^2P_{1/2}^e$	29.06	29.1	65.0	23.7
$5s^25p^4(^3P)6d\ ^4P_{1/2}^e$	29.33			
$5s^25p^4(^1D)6d\ ^2P_{1/2}^e$	31.27			
$5s^25p^4(^3P)8s\ ^4P_{1/2}^e$	31.40	31.5	22.9	9.3
$5s^25p^4(^1D)6d\ ^2S_{1/2}^e$	31.47			
$5s^25p^4(^3P)8s\ ^2P_{1/2}^e$	31.64			
$5s^25p^4(^1D)7d\ ^2P_{1/2}^e$	32.85			
$5s^25p^4(^1D)7d\ ^2S_{1/2}^e$	32.91	32.85	9.7	3.3
$5s^25p^4(^1D)7s\ ^2S_{1/2}^e$	33.04			
$5s^25p^4(^1D)8d\ ^2S_{1/2}^e$	33.6	34.1	8.9	4.3
$5s^25p^4(^1D)8d\ ^2P_{1/2}^e$	33.7			
$Xe^{2+} + e$		$35 \leq \epsilon < 45$	21.2	14.1

<sup>a</sup>Configuration and optical energy based on the tabulation of Ref. [19].

manifold by some workers [6]. The most obvious candidate for these transitions is the  $5p$  manifold. There are, however, no suitable final states of odd parity near 25.3 eV. There are, instead, several states near 25.3 eV belonging to the  $d$  manifold. These are, in  $LS$  notation, the  $5s^2 5p^4 ({}^3P) 5d^2 D_{3/2}^e$ ,  $({}^1D) 6s^2 D_{5/2}^e$ , and  $({}^1D) 6s^2 D_{3/2}^e$  states at 25.19, 25.71, and 26.13 eV, respectively. These even-parity states can only be excited through  $d$ -wave correlations in the Xe ground-state wave function. It is interesting to note that McCarthy *et al.* [2], in their accurate EMS study of argon, established a  $d$ -wave transition to the  $3s^2 3p^4 ({}^1D) 4s^2 D^e$  argon ion states. This is the only  $d$ -wave transition observed in argon and its momentum profile provides a sensitive test of ground-state correlations. The cross section for an  $nd^{-1}$  transition has a minimum at  $p=0$  and rises as  $p$  (and  $\phi$ ) increases. This fits the present data (Table I). This transition therefore probably belongs to the  $nd$  manifold, and its relative intensity and momentum profile (discussed below) provides detailed information on the ground-state correlations.

Concerning the 26.5-eV transition, Hansen and Persson [18,19] correctly assign this to the  $5p$  manifold. The probable final states are the  $5s^2 5p^4 ({}^3P) 6p^2 P^o$  states with a weighted centroid energy of 26.48 eV. It is interesting to note that McCarthy *et al.* [2] observed the corresponding transition  $3s^2 3p^4 ({}^3P) 4p^2 P^o$  in argon with an intensity of 0.01 of the total  $3p$  manifold cross section. They also saw a stronger  $3p^{-1}$  transition with 0.03 of the manifold cross section leading to the  $3s^2 3p^4 ({}^1D) 4p^2 P^o$  ion state. The corresponding (weighted mean) transition in xenon is at 28.34, as can be seen in Table I. This latter transition, which will be discussed in detail below, is masked by the much stronger  $5s^{-1}$  transitions at around 28 eV (Table I). The  $5s^2 5p^4 ({}^1D) 6p^2 P^o$  final state is also expected to be the most dominant  $5p^{-1}$  satellite line according to the calculation of Dyall and Larkins [16]. The remaining peaks, as well as the intensity in the continuum above the double ionization threshold of 33.1 eV, belong largely to the  $5s$  manifold.

### B. Momentum distributions

Separation-energy spectra similar to those shown in Fig. 1 were taken at a range of azimuthal angles. The energy range at each angle and the angular range itself were stepped through repeatedly. Each part of each spectrum at every angle was scanned sequentially for an equal time, each run consisting of many scans. The spectra were then used to obtain cross sections to selected final ion states relative to each other as a function of  $\phi$  or momentum  $p$ . In some cases neighboring final ion states could not be resolved; where this occurred they were then grouped under single peaks.

The measured angular correlations (or momentum profiles) are not absolute, but relative normalizations are maintained. The present momentum profiles are normalized to the DWIA by equating the measured intensity at  $\phi=7.5^\circ$  ( $p=0.56$  a.u.) in the  $5p$  ground-state transition to the DWIA value at that point. The DWIA-TDFA (and THFA) calculations were taken from the work of Cook *et al.* [5]. Nearly all of the  $5p$  strength goes to the

ground-state transition. This can be seen from Table I. In the present measurements we find the spectroscopic factor for the ground-state transition to be  $0.96 \pm 0.02$ , and we have taken this into account in the normalization of the current data.

Figure 2 shows that the DWIA cross section for the  $5s$  manifold (open circles) is in excellent agreement with the measured  $5s$  manifold cross section both in shape and in magnitude at small angles where the cross section peaks. This shows that essentially all of the  $5s$  strength has been observed in the measurement over the range 23–45 eV. Nearly all of the strength in this region belongs to the  $5s$  manifold; the small  $5p$  and  $nd$  strengths which are observed and discussed below are not included in the  $5s$  manifold cross section shown in the figure. It is interesting to note that agreement in magnitude is only obtained if the Dirac-Fock wave functions are used to describe the  $5s$  and  $5p$  transitions. The nonrelativistic HF wave functions lead to much poorer agreement, the main effect being the significant overestimate of the  $5s$  cross section at low momenta  $p$ , i.e., at small angles  $\phi$ . The DWIA-TDFA is thus our preferred calculation and consequently it is to this that we refer in all subsequent discussion.

It is interesting to note that the calculations underestimate the cross section at angles above about  $8^\circ$ , corresponding to momenta above about 0.6 a.u. This is

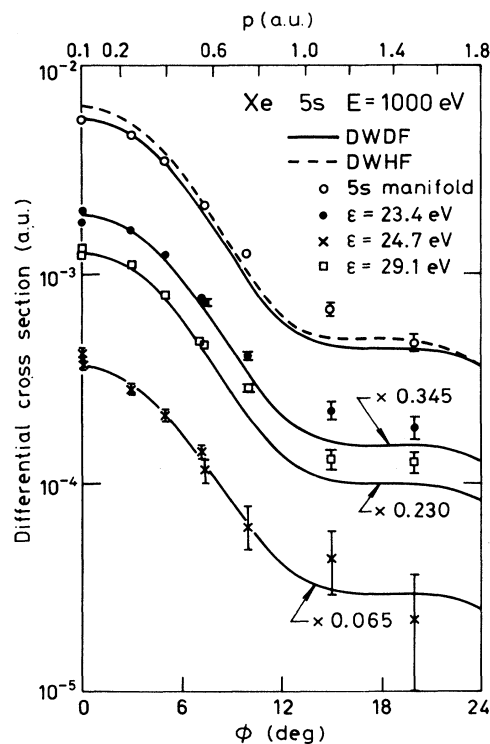


FIG. 2. The 1000-eV noncoplanar symmetric momentum profiles for the first excited state at 23.4 eV, the state at 24.7 eV, the group peaked at 29.1 eV, and the total  $J^\pi = \frac{1}{2}^+$  manifold compared with DWIA using DF (solid line) and HF (dashed line)  $5s$  wave functions. All data have been normalized by fitting the measured ground-state transition at  $\phi=7.5^\circ$  to 0.96 times the  $5p$  DWDF cross section.

highlighted by the log plot. This implies that the calculation may underestimate the role of distortion, which tends to be more serious at high momenta [1], although it does give the correct  $5p$ - $5s$  manifold cross-section ratio.

The shape of the 23.4-eV transition is indistinguishable from the  $5s$  manifold cross section. It is in similar agreement with the DWIA-DF calculation, as is its magnitude, when the calculated manifold cross section is multiplied by the factor of 0.345 (Fig. 2). Thus the spectroscopic factor [Eq. (6)] for this transition is 0.345. The 23.4-eV state with dominant configuration of  $5s5p^6$  therefore contains only about one-third of the  $5s$  pole strength.

Figure 2 also shows the momentum profiles for the transitions centered about 24.7 and 29.1 eV. These also obviously belong to the  $5s$  manifold with strengths of 0.065 and 0.23, respectively. We note that the shapes for the 23.4-, 24.7-, and 29.1-eV transitions are identical within experimental error.

Figure 3 shows the momentum profiles observed for the transitions centered about 28.0, 31.5, 32.85, and 34.1 eV. Again, all show the same shape as the other  $5s$  manifold transitions, and thus they must belong to the  $5s$  manifold. The 28.0-eV transition could also include transitions to the odd-parity ion states  $5s^25p^4(^1D)6p^2P_{1/2}^o$  and  $^2P_{3/2}^o$  at 28.21 and 28.59 eV [19], respectively. The corresponding  $3s^23p^4(^1D)4p$  states in argon were found by McCarthy *et al.* [2] to give the dominant  $3p$  satellite contribution, accounting for 0.03 of the  $3p$  manifold strength. The present measurements give an upper limit

of 0.01 for the combined  $5p$  spectroscopic strength of these two  $^2P^o$  final states.

The transitions in the regions centered about 32.85 and 34.1 eV have been combined in Fig. 2. They are of equal strength (0.035 each). The latter transition is in the continuum, i.e., above the  $\text{Xe}^{2+} + 2e$  threshold of 33.1 eV.

The momentum profile of the cross section in the continuum between 35 and 45 eV is shown in Fig. 4. The peak in this cross section is not at  $0^\circ$ , which indicates the presence of a  $5p$  component, although the large cross section at  $0^\circ$  indicates that the  $5s$  manifold still dominates in the continuum. An excellent fit to the data is obtained by assuming both  $5s$  and  $5p$  transitions contribute, the integrated  $5s$  and  $5p$  spectroscopic strengths being 0.08 and 0.03, respectively (Fig. 4).

The spectroscopic factors for final states belonging to the  $5s$  manifold can be obtained from the momentum profiles (Fig. 2-4) as well as from the relative intensities (Table I) obtained from the energy spectra (Fig. 1). The results are given in Table II, where they are also compared with two recent  $(\gamma, e)$  results [6,8] and a recent theoretical calculation [20].

The agreement between the present EMS spectroscopic factors and those of Cook *et al.* [5] at 1000 and 1200 eV, within the uncertainties on the respective data sets, is generally good. We note that the major discrepancy between the present EMS study and that of Cook *et al.* [5] in  $S_f$  is for the transition at 25.3 eV, although the values

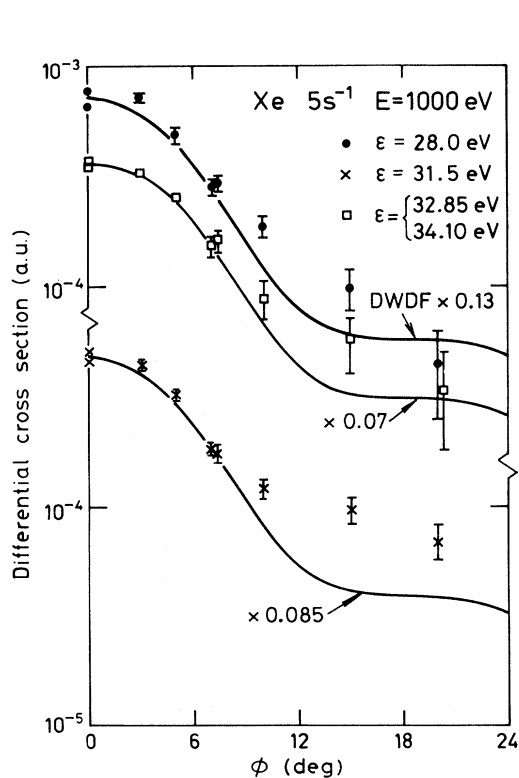


FIG. 3. Momentum profiles for the indicated transitions compared with calculated  $5s$  DWDF profiles multiplied by the respective spectroscopic factors.

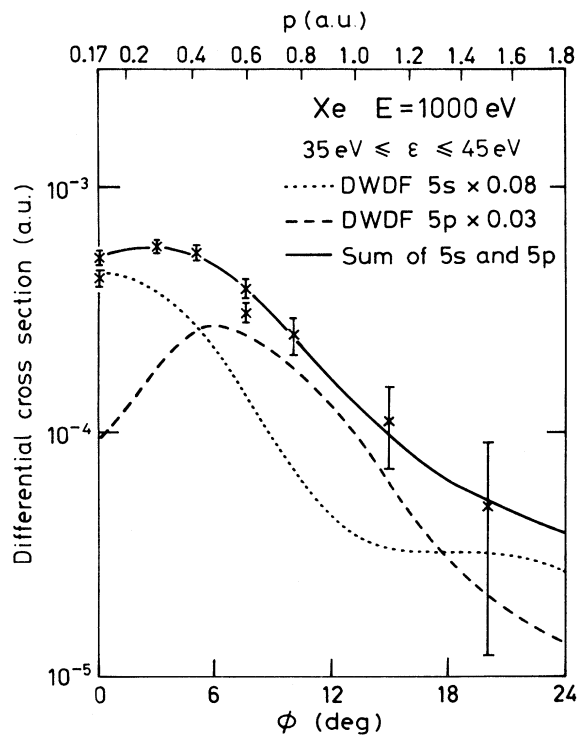


FIG. 4. The momentum profile observed in the continuum between 35 and 45 eV compared with the calculated DWDF momentum profiles. Both  $5s$  and  $5p$  contributions are required; the respective spectroscopic factors are indicated.

of  $S_f$ , for this transition, of the present study and Cook *et al.* [5] are both small and have quite large uncertainties. Nonetheless, we ascribe this discrepancy as being due to the earlier work having significantly poorer energy resolution, particularly at 1200 eV, than the present study, which meant that they might not necessarily extract the correct values of  $S_f$  from their measured separation-energy spectra. Furthermore, this is also why Cook *et al.* [5] incorrectly assigned the small 25.3- and 26.5-eV transitions to the  $5s$  manifold. We also note that there is a serious disagreement between the PES and EMS results. Part of this is due to the difficulty of identifying the continuum contribution in PES measurements. The major difference has, however, been explained by Kheifets and Amusia [15,20] as being due to the role of initial-state correlation effects in the high-momentum PES measurements. Such effects are absent in the low-momentum ( $\leq 1$  a.u.) EMS measurements, which obtain the true spectroscopic factor as defined by Eq. (6). Kheifets and Amusia [20] found that if they corrected the spectroscopic factors for the high-momentum initial-state correlation effects, they obtained good agreement with the high-energy PES measurements of Svensson *et al.* [6]. Their calculated spectroscopic factors, based on a relativistic Green's-function many-body calculation, are in quite good agreement with the EMS data. We note that their spectroscopic factors depend sensitively on the energies

used for the  $5p^4(^3P)nl$   $LS$  ion states. However, their choice of the value from Moore [28] for  $\epsilon_{5p^4(^3P_2)}$ , instead of that which they calculated from the Dyson equation solution, is not unreasonable and was certainly not made to ensure agreement with any experimental spectroscopic factors [29]. Furthermore, inclusion of relativistic effects allowed them to describe the  $J^\pi = \frac{1}{2}^+$  ion states not of  $^2S$  symmetry. Within their nonrelativistic scheme the primary  $5s$  vacancy is allowed to interact directly with the  $5s^2 5p^4(^1D)nd$   $^2S$  ion states, which are spread over relativistic  $5p^4nl$   $J^\pi = \frac{1}{2}^+$  eigenvectors. This allowed them to take into account explicitly the continuous  $5p^4nd$  excitations rather than using pseudostates, as in Ref. [5]. They also included in their model part of the direct interaction between two  $5p$  holes and an  $nd$  excited electron. This takes into account a broader class of many-electron correlations in the final ionic state as compared to the standard configuration-interaction technique.

Cook *et al.* [5] carried out detailed relativistic configuration-interaction calculations on the target xenon atom and residual ion states in order to identify causes of the complex structure associated with the  $5s$  manifold. They found that the inclusion of relativistic effects in their calculations lowered the spectroscopic factor for the "main" 23.4-eV transition by about 0.1. Even so, the lowest spectroscopic factor for this transition obtained in

TABLE II. Comparison of spectroscopic factors for  $J = \frac{1}{2}^+$  ion states belonging to the  $5s$  manifold of xenon. The error in the last significant figure is given in parentheses.

Present (EMS)			$(\gamma, e)$				Theory (Ref. [20])		
Main configuration	$\epsilon_f$ (eV)	$S_f$	Main configuration	$\epsilon_e$ (eV) <sup>a</sup>	$S_f^a$	$S_f^b$	Main configuration	$\epsilon_f$ (eV)	$S_f$
$5s5p^6^2S$	23.4	0.345(10)	$5s5p^6^2S$	23.4	0.48	0.56	$5s5p^6^2S$	23.22	0.38
$5s^2 5p^4(^3P)6s^4P$	24.7	0.065(8)	$(^3P)6s^4P$	24.63	0.03	0.04	$(^3P)5d, 6s^4P, ^2P$	24.49	0.07
$5s^2 5p^4(^3P)5d^2P$							$(^3P), (^1D)5d^2P$	24.68	
$5s^2 5p^4(^3P)5d^4P$	25.3	< 0.005	$(^3P)5d^4P$	25.29	0.03	0.05	$(^3P)6s^2P$	25.15	0.06
$5s^2 5p^4(^3P)6s^2P$							$(^3P)6s^4P$	25.54	
$5s^2 5p^4(^1D)5d^2P$			$(^1D)5d^2P$	27.82			$(^1S)6s^2S$	28.19	
$5s^2 5p^4(^1S)6s^2S$	28.0	0.125(8)	$(^1S)6s^2S$	28.22	0.10	0.06	$(^3P)6d, 5d^2P$	28.70	0.06
							$(^3P)6d^4P$	28.97	
$5s^2 5p^4(^1D)5d^2S$			$(^1D)5d^2S$	28.71			$(^3P)6d^4P, ^2P$	29.49	
$5s^2 5p^4(^3P)6d^2P$	29.1	0.230(8)	$(^3P)6d^2P$	29.08	0.24	0.12	$(^1D)5d^2S$	29.50	0.23
$5s^2 5p^4(^3P)6d^4P$			$(^3P)6d^4P$	29.44			$(^3P)7d^4P$	30.60	
			$(^3P)7d^4P, ^2P$	30.67			$(^3P)7d^2P$	30.71	
$5s^2 5p^4(^1D)6d^2P$			$(^1D)6d^2S, ^2P$	31.44					
$5s^2 5p^4(^1D)6d^2S$	31.5	0.085(7)	$(^3P)8s^4P$	31.90	0.08	0.07	$(^1D)6d^2S, ^2P$	31.57	0.09
$5s^2 5p^4(^3P)8s^4P, ^2P$									
$5s^2 5p^4(^1D)7d^2S, ^2P$	32.85	0.035(6)	$(^1D)7d^2S, ^2P$	32.81			$(^1D)7d^2S$	32.87	
$5s^2 5p^4(^1D)8d^2S$					0.03	0.04	$(^1D)8d^2S$	33.60	0.06
$5s^2 5p^4(^1D)9d^2S$	34.1	0.035(6)	$(^1D)8d^2S, ^2P$	33.50			$(^1D)9d^2S$	34.05	
$Xe^{+2} + e$	$\geq 35$ < 45	0.08(2)					Continuum		0.07
$\epsilon_{5s}$ (center of gravity)	$28.0 \pm 0.3$			26.3				27.5	

<sup>a</sup>Reference [6] ( $E_\gamma = 1487$  eV).

<sup>b</sup>Reference [8] ( $E_\gamma = 80$  eV).

their best calculation was 0.48, significantly higher than the measured value (0.35) and the value calculated by Kheifets and Amusia (0.38). They did note, however, that the more exact the many-body calculation was the lower became the value of the spectroscopic factor for this transition.

Table II also lists the  $5s$  orbital energy obtained from the measurements by application of Eq. 8. The present value of  $28.0 \pm 0.3$  eV agrees well with the value of  $27.6 \pm 0.3$  eV obtained by Cook *et al.* [5] and with the Dirac-Fock value of 27.49 eV [5,20]. The HF orbital energy of 25.70 eV is much lower, as is that given by the PES measurements (26.3 eV).

We now turn to transitions which do not belong to the  $5s$  manifold. Figure 5 shows on a linear scale the momentum profiles for the 25.3- and 26.5-eV transitions. Their shape is quite different than that for the  $5s$  transitions, and they cannot therefore belong to the  $5s$  manifold.

In the region near 26.5 eV several final states are possible candidates (Table I). The most obvious are the 26.23- and 26.61-eV ( $^3P$ ) $^2P_{1/2,3/2}^o$  states. Transitions to these odd-parity states must belong to the  $p$  manifold. Figure 5(b) shows that the  $5p$  momentum distribution indeed gives an excellent fit to the data, both in shape and in magnitude, when multiplied by the factor of 0.02. These transitions have normally been mistakenly assigned to the  $5s$  manifold in PES work [6,8,9]. They were, however, tentatively identified by Hansen and Persson [18] as belonging to the  $5p$  manifold on the basis of PES satellite intensity measurements at low photon energy [24,25].

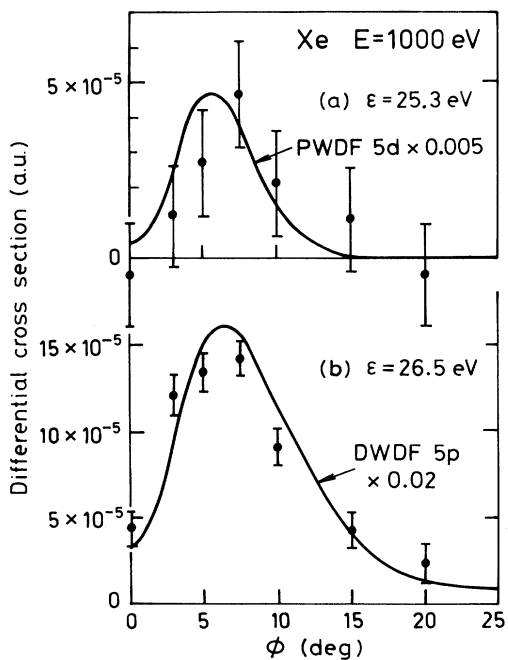


FIG. 5. The momentum profiles observed to final states centered around 25.3 and 26.5 eV compared with calculated DF  $5d$  and  $5p$  momentum profiles multiplied by the respective spectroscopic factors. The  $5d$  cross section is obtained using the PWIA.

The present results clearly support this assignment.

In the region around 25.3 eV [Fig. 5(a)] there are no suitable  $J = \frac{1}{2}, \frac{3}{2}$  odd-parity final states [19]. Thus this transition cannot be assigned to the  $5p$  manifold, although its shape is in very good agreement with that expected for a  $5p$  transition. It has been assigned in previous EMS [5] and PES [6,8,9] measurements to the  $5s$  manifold. The shape of the cross section excludes any  $5s$  manifold contribution. The only remaining possibility is that it could belong to the  $nd$  manifold. This can only arise if there are  $d$ -wave correlations in the initial ground state. Possible final ion states are the  $5s^2 5p^4 ({}^3P) 5d^2 D_{3/2}^e$  state at 25.19 and the  $({}^1D) 6s^2 D_{5/2,3/2}^e$  states at 25.71 and 26.13 eV (Table I).

It is interesting to note that in their high-resolution EMS study of argon, McCarthy *et al.* [2] were able to identify a  $d$ -wave transition leading to the  $3s^2 3p^4 ({}^1D) 4s^2 D^e$  argon ion states. This strongly suggests that the corresponding states in xenon mentioned above are indeed the ones involved in the transition shown in Fig. 5(a).

The observed momentum distribution for the 25.3-eV transition [Fig. 5(a)] is similar to that observed for the 26.5-eV transition. In fact it can be well fitted by the  $5p$  momentum profile with a strength of 0.005. However, as discussed above, there are no suitable odd-parity states in the region of interest.

Assuming, as in argon, that there are small  $d$ -wave components in the xenon ground state, the most dominant  $d$ -wave contribution is likely to come from the  $5s^2 5p^4 5d^2$  configuration. On this basis one should observe a  $d$ -wave momentum profile dominated by the  $5d$  orbital. The calculated momentum profile in Fig. 5(a) shows the plane-wave impulse DF approximation  $5d$  cross section based on two target electrons excited to the  $5d$  orbital. It has been multiplied by the factor of 0.005. The shape is in very good agreement with the measured profile, and such a small  $d$ -wave admixture in the ground state is quite reasonable. Cook *et al.* [5], in their relativistic configuration-interaction calculations, found that the sum total of the strength of the  $\frac{3}{2}^+$  and  $\frac{5}{2}^+$  manifolds was less than 1% of the strength of the  $\frac{1}{2}^+$  manifold for  $p < 0.8$  a.u. The present measurements are quite consistent with this result.

If the  $5s^2 5p^4 5d^2$  configuration contains most of the  $d$ -wave strength in the ground state, the most likely transition would be to the  $5s^2 5p^4 5d^2 D_{3/2}^e$  ion state at 25.2 eV. This is indeed where Svensson *et al.* [6], Brion, Bawagan, and Tan [8], Fahlman, Krause, and Carlson [24], Süzer and Hush [25], and Carlsson-Göthe, Baltzer, and Wannberg [26] find significant strength in their high-resolution PES measurements. Hansen and Persson [18], in their analysis of the low-energy PES results of Fahlman, Krause, and Carlson [24] and Süzer and Hush [25], find that they cannot allocate the observed satellite at 25.3 eV to the  ${}^2P^o$  manifold since there are no odd-parity final states of the required energy, nor was the behavior of the satellite intensity consistent with an assignment to the  $5s$  manifold. This supports the present assignment to the  $d$  manifold. If the final state is this  $J^\pi = \frac{3}{2}^+$  ion state, it is natural to assume that the  $5s^2 5p^4 5d^2 D_{5/2}^e$  ion state

TABLE III. Spectroscopic factors for the  $^2P^o$  manifold of  $\text{Xe}^+$  compared with several calculations. The error in the last significant figure is given in parentheses.

Dominant configuration	$\varepsilon$ (eV)	Present EMS	Theory		
			Complete <sup>a</sup>	Overlap <sup>b</sup>	FSCI <sup>a</sup>
$5s^25p^5^2P^o_{3/2}$	12.13	0.96(2)	0.980	0.976	0.931
$5s^25p^5^2P^o_{1/2}$	13.43		0.983		0.927
$5s^25p^4(^3P)6p^2P^o_{1/2}$	26.23				
$5s^25p^4(^3P)6p^2P^o_{3/2}$	26.61	0.012(8)		0.002	
$5s^25p^4(^1D)6p^2P^o_{3/2}$	28.21				
$5s^25p^4(^1D)6p^2P^o_{1/2}$	28.59	< 0.01		0.012	
Continuum		0.03(1)			

<sup>a</sup>Reference [5]; relativistic CI. FSCI denotes final-state configuration interaction.

<sup>b</sup>Reference [16]; nonrelativistic CI.

at 26.36 eV should also be excited. Fahlman, Krause, and Carlson [24] and Süzer and Hush [25] both see excitation of a state at 26.3 eV. Carlsson-Göthe, Baltzer, and Wannberg [26], in their very-high-resolution study, using monochromatized He II $\alpha$  radiation, find very strong excitation of this state at 26.36 eV, the intensity being nearly an order of magnitude greater than that for the  $5s^{-1}$  transition to the state at 24.67 eV.

Transitions to this final state would contribute to the 26.5-eV peak. The shape of both the  $d$ -wave and  $p$ -wave transitions are essentially identical [Figs. 5(a) and 5(b)], and it is therefore not possible to exclude a  $d$ -wave contribution to the peak centered at 26.5 eV. Based on the 25.3-eV cross section, which is likely to be dominated by the transition to the  $(^3P)5d^2D_{3/2}$  state at 25.2 eV [24–26], it is quite possible that up to about one-third of the 26.5-eV cross section could be contributed by a  $d$ -wave transition to the  $(^3P)5d^2D_{5/2}$  state at 26.3 eV.

It is now possible to evaluate the spectroscopic factors for the  $5p$  manifold. They are given in Table III, where they are also compared with several theoretical calculations. The  $5p$  manifold, unlike the  $5s$ , is almost a pure one-hole state with essentially all of the strength contained in the ion ground state. This is reproduced by the many-body calculations [5,16] and supported by the present results. Finally we note (see Table III) that Cook *et al.* [5] found the quite interesting result that if only final-state electron correlations are allowed for, the spectroscopic factor (i.e., the one-hole nature) of the final state is actually lower than that obtained if correlations are also included in the initial state.

## V. SUMMARY

Accurate EMS measurements at 1000 eV have been made for transitions to excited states of  $\text{Xe}^+$  as well as to the continuum. The momentum profiles and cross sections relative to the ground-state  $5p^{-1}$  transition are accurately described by the distorted-wave impulse approximation. Detailed spectroscopic factor determinations have been obtained for the  $5s$  manifold. The main  $5s$  transition at  $\varepsilon=23.4$  eV has a spectroscopic strength of 0.345. This is in very good agreement with the previous

less accurate measurements of Cook *et al.* [5] as well as with the most recent theoretical calculations, including relativistic effects of Kheifets and Amusia [20]. Spectroscopic factors for the  $5s$  manifold are correctly determined by comparing cross sections for states within the manifold, the sum of the different  $5s$  components giving the correct  $5s$  manifold cross section normalized relative to the  $5p$  cross section. The PES data obtain spectroscopic factors different than those obtained in EMS. At low energies the PES relative intensities are sensitive functions of the energies and depend on the reaction dynamics. At high energies they probe the high-momentum regions of the target state correlation effects. As Amusia and Kheifets explained, it is necessary to correct these high-recoil-momentum spectroscopic factors to obtain true spectroscopic factors. Thus comparison between EMS and PES or structure calculations with PES spectroscopic strength is not straightforward.

The present measurements reveal significant  $5p$  strength in the continuum. They also show a somewhat smaller  $5p$  spectroscopic strength to final ion states around 26.5 eV. They confirm that the  $5p^{-1}$  ground-state transition is almost a pure one-hole transition with a spectroscopic factor of  $0.96\pm 0.02$ . This is verified in the detailed multiconfiguration Dirac-Fock optimal level of the atom and ion ground states by Cook *et al.* [5].

We have observed transitions belonging to the  $^2D^e_{3/2,5/2}$  manifold. These can only occur if there are  $d$ -wave correlations in the xenon ground state. The observed momentum distribution is well described by the DF  $5d$  wave function, suggesting that the target electron is knocked out of a  $5d$  orbital in a  $5s^25p^45d^2$  ground-state component. The strength of this component needs to be only 0.005 in order to explain the observed cross section.

## ACKNOWLEDGMENTS

We are grateful to the Australian Research Council for financial support of this work and to Ian McCarthy for carrying out the calculation of the  $5d$  momentum distribution. One of us (M.B.) also acknowledges the ARC for additional support.

- [1] I. E. McCarthy and E. Weigold, *Rep. Prog. Phys.* **51**, 299 (1988); **54**, 789 (1991).
- [2] I. E. McCarthy, R. Pascual, P. Storer, and E. Weigold, *Phys. Rev. A* **40**, 3041 (1989).
- [3] K. T. Leung and C. E. Brion, *Chem. Phys.* **82**, 87 (1983).
- [4] A. Ugbabe, E. Weigold, and I. E. McCarthy, *Phys. Rev. A* **11**, 576 (1975).
- [5] J. P. D. Cook, I. E. McCarthy, J. Mitroy, and E. Weigold, *Phys. Rev. A* **33**, 211 (1986).
- [6] S. Svensson, B. Erikson, N. Mårtensson, G. Wendin, and U. Gelius, *J. Electron Spectrosc. Relat. Phenom.* **47**, 327 (1988).
- [7] M. Y. Adam, F. Wuilleumier, N. Sandner, V. Schmidt, and G. Wendin, *J. Phys. (Paris)* **39**, 129 (1978).
- [8] C. E. Brion, A. O. Bawagan, and T. K. Tan, *Can. J. Chem.* **66**, 1877 (1988).
- [9] S. Svensson, K. Heleneberg, and U. Gelius, *Phys. Rev. Lett.* **58**, 1624 (1987).
- [10] R. L. Martin, S. P. Kowalczyk, and D. A. Shirley, *J. Chem. Phys.* **68**, 3829 (1978).
- [11] M. Ya. Amusia and A. S. Kheifets, *J. Phys. B* **18**, L679 (1985).
- [12] J. Mitroy, K. Amos, and I. Morrison, *J. Phys. B* **17**, 1659 (1984).
- [13] A. Hibbert and J. E. Hansen, *J. Phys. B* **20**, L245 (1987).
- [14] J. E. Hansen, *J. Opt. Soc. Am.* **67**, 754 (1977).
- [15] M. Ya. Amusia and A. S. Kheifets, *Aust. J. Phys.* **44**, 293 (1991).
- [16] K. G. Dyall and F. P. Larkins, *J. Phys. B* **15**, 219 (1982).
- [17] J. E. Hansen and W. Persson, *Phys. Rev. A* **18**, 1459 (1978).
- [18] J. E. Hansen and W. Persson, *Phys. Rev. A* **30**, 1565 (1984).
- [19] J. E. Hansen and W. Persson, *Phys. Scr.* **36**, 602 (1987).
- [20] A. S. Kheifets and M. Ya. Amusia, *Phys. Rev. A* **46**, 1261 (1992).
- [21] J. Mitroy, I. E. McCarthy, and E. Weigold, *J. Phys. B* **18**, L91 (1985).
- [22] A. S. Kheifets, *Zh. Eksp. Teor. Fiz.* **89**, 459 (1985) [*Sov. Phys. JETP* **62**, 260 (1985)].
- [23] J. P. D. Cook, J. Mitroy, and E. Weigold, *Phys. Rev. Lett.* **52**, 1116 (1984).
- [24] A. Fahlman, M. O. Krause, and T. A. Carlson, *J. Phys. B* **17**, L217 (1984).
- [25] A. Süzer and N. S. Hush, *J. Phys. B* **10**, L705 (1977).
- [26] M. Carlson-Göthe, P. Baltzer, and B. Wannberg, *J. Phys. B* **24**, 2477 (1991).
- [27] M. O. Krause, S. B. Whitfield, C. D. Caldwell, J.-Z. Wu, P. van der Meulen, C. A. de Lange, and R. W. C. Hansen, *J. Electron Spectrosc. Relat. Phenom.* **58**, 79 (1992).
- [28] C. E. Moore, *Atomic Energy Levels*, Natl. Bur. Stand. (U.S.) Circ. No. 467 (U.S. GPO, Washington, DC, 1958), Vol. III.
- [29] A. S. Kheifets (private communication).